

Three-Axis Attitude Determination Using Global Positioning System Signal Strength Measurements

E. Glenn Lightsey* and Jared Madsen†

University of Texas at Austin, Austin, Texas 78712-1085

An alternative method to the standard carrier-phase algorithm for deriving three-axis attitude solutions from global positioning system (GPS) signal sources is investigated. This new method uses signal-to-noise ratio (SNR) measurements from two or more canted antennas and a knowledge of each receiving antenna's gain pattern to generate pointing vector solutions. These vector solutions are then converted to a three-axis attitude solution. The method has the advantage of requiring no complicated initializing procedures such as integer ambiguity resolution, and it can generate three-axis solutions with as few as two antennas. A solution is produced whenever a minimum of three GPS satellites are in view, regardless of the vehicle's orientation at that time or at any time previously. The performance of this SNR approach is investigated using a Kalman filter to derive solutions on a satellite whose attitude generally remains fixed in the local frame. The performance of the algorithm is evaluated while the canting angles between the antennas and the filter values are varied. In addition, self-calibrating and self-scaling options are explored to reduce the algorithm's dependence on any outside knowledge of the vehicle's attitude during an in-flight calibration process. The study also examines the performance of the solution under the expected error conditions of an inaccurate calibration and sky blockage. The results demonstrate that the estimate is relatively insensitive to these expected errors. Some general conclusions are drawn about the performance and sensitivity of the developed algorithm.

Introduction

GLOBAL positioning systems (GPS) have found widespread use on spacecraft to provide both position and attitude information. These systems have the advantage of being relatively inexpensive and accurate. GPS systems generally derive attitude solutions by using an array of three or more antennas in a precisely known layout. When highly accurate carrier-phase measurements are taken between antennas and various GPS satellites, attitude solutions can be generated. This method has been previously employed on spacecraft and has demonstrated accuracies to the subdegree level in the presence of measurement noise for antenna separations of 1 m or more.^{1–7} Although suitable for some applications, this approach has shortcomings. Although the solutions the method generates are highly accurate, they are not highly robust. To generate a solution, the receiver must perform a process known as integer ambiguity resolution. This process is complex and susceptible to failure. For example, one algorithm assumes that the antenna array is pointed within 15 deg of zenith during the integer ambiguity resolution process.⁸ If it is not within this range, the process will fail, and no solutions will be generated.

An alternative method for estimating the pointing vector of a space-based platform has previously been developed.⁹ This method utilizes signal-to-noise measurements from various GPS satellites and a knowledge of the gain pattern of the receiving antenna. This method has the advantage of requiring no ambiguity resolution, and it uses minimal memory and time to implement. To have sufficient knowledge of the gain pattern to generate the most accurate solutions, however, a calibration process is required for the antenna used. Because of the limitations in the measurement accuracy of the signal-to-noise ratio (SNR), this method generally only provides unfiltered solutions accurate to within 30 deg of truth, even

when a calibration has been performed. Additionally, because gain patterns typically have minimal variance in the azimuth direction, single-antenna solutions generated by this technique provide no information in that direction. In attitude solution terminology, these solutions will provide pitch and roll information, but not yaw.

This solution approach was first explored by Axelrad and Behre to generate single-pointing vector solutions.¹⁰ Dunn and Duncan used a similar technique to obtain point vector solutions that were accurate to within 15 deg on the Microlab-1 satellite.¹¹ Full three-axis attitude solutions were computed by Buist et al.¹² using a single antenna on a gravity gradient stabilized satellite known as PoSAT-1. In this case, the presence of a gravity gradient boom created variation in the azimuthal gain pattern of the antenna, which was combined with the gravity gradient dynamics to generate solutions that agreed to within 10 deg of those derived independently using a magnetometer.¹² Full attitude solutions from a single GPS antenna are generally not possible, however, because the gain pattern of a hemispherical antenna typically has little or no variation in the azimuth direction and the knowledge of the vehicle dynamics may be limited.

Serrano et al.¹³ developed an SNR algorithm that determined attitude solutions from multiple antennas. In their work, common satellites visible to two canted antennas and the resulting vector observations were used to compute the attitude rotation matrix by solving Wahba's problem.¹⁴ Serrano et al.¹³ determined that such a system could be accurate if the SNR modeling was also accurate. Another noncarrier wave attitude determination system has been presented by Pasetti et al.¹⁵ This method uses sets of visible, nonvisible, and potentially visible satellites to determine vehicle attitude with multiple antennas. The antenna arrays analyzed by Pasetti et al. consisted of antennas pointing in the zenith, nadir, front, and aft directions. These types of arrangements could be problematic if a carrier-phase method is to be used in tandem with the noncarrier wave methods because carrier-phase methods require single satellites to be visible by multiple antennas.

This paper investigates the extension of the SNR theory presented by Axelrad and Behre¹⁰ to multiple canted antennas to generate full three-axis attitude solutions in a manner similar to that done by Serrano et al.¹³ This work further expands on these methods by using high-integrity orbit simulations in tandem with actual GPS receiver hardware to investigate likely system accuracies and error sensitivities. The value of using more than two canted antennas is investigated and tested. The effects of inaccurate calibration and sky

Received 4 December 2001; revision received 12 July 2002; accepted for publication 5 December 2002. Copyright © 2003 by the American Institute of Aeronautics and Astronautics, Inc. All rights reserved. Copies of this paper may be made for personal or internal use, on condition that the copier pay the \$10.00 per-copy fee to the Copyright Clearance Center, Inc., 222 Rosewood Drive, Danvers, MA 01923; include the code 0731-5090/03 \$10.00 in correspondence with the CCC.

*Assistant Professor, Department of Aerospace Engineering and Engineering Mechanics. Senior Member AIAA.

†Ph.D. Candidate, Department of Aerospace Engineering and Engineering Mechanics.

blockage are also investigated to demonstrate the robustness of this new algorithm.

The solutions generated by this method may be used to initialize the more accurate carrier-phase methods of attitude determination more quickly than traditional integer ambiguity search methods. These solutions may also be used when the more accurate solutions are not available.

Single-Vector Solution Approach

The basis of the SNR approach is that a pointing vector solution can be generated from one receiving antenna because the gain pattern of the receiving antenna is approximately known and is invariant in the antenna body frame. For hemispherical antennas, the gain pattern is typically similar to the behavior of a cosine function and is primarily a function of the antenna boresight offset angle. As a signal source travels from directly overhead the antenna toward a 90-deg offset, the SNR will correspondingly start at a maximum value and then drop toward zero. In some instances, GPS satellites may even be tracked below the horizon of the antenna. When either a calibration curve or this simple cosine model is used, the angle between the antenna boresight vector and the line-of-sight vector to the signal source can be estimated from a given SNR measurement. If the line-of-sight vector is normalized to a unit vector, then the equation to determine the pointing vector solution is the dot product

$$\mathbf{B} \cdot \mathbf{L} = \cos \alpha = B_x L_x + B_y L_y + B_z L_z \quad (1)$$

In Eq. (1), \mathbf{B} is the unit normal antenna boresight vector, \mathbf{L} is the line-of-sight vector from the receiver antenna to the signal source, and α is the angle between these two vectors (Fig. 1).

With the presented measurement model, the three components of \mathbf{L} can be found in the external reference frame if the location of the antenna and the signal source are known, that is, both the receiver position and the GPS satellite positions are known. For a given SNR measurement, $\cos(\alpha)$ can be determined from the calibration function, and \mathbf{B} can, therefore, be determined from as few as three measurements. This model assumes that the only variable affecting the SNR measurement is the offset angle to the antenna boresight vector, whereas in fact other parameters will also affect the measurement. Namely, variations in the gain pattern of the antenna over the azimuth direction, multipath, and signal strength loss due to distance from the GPS satellite may all impact the measurement. These effects generally are smaller than the noise seen in the SNR measurement, however, and no significant improvement is expected from incorporating them into the measurement model. Further research is underway to verify this assumption.

To generate single-vector solutions, the line-of-sight vector is required. This is readily available from a GPS receiver once a position fix has been obtained. A position fix, however, requires four measurements, whereas the pointing vector algorithm requires only three. If only three measurements are available, it is still possible to generate line-of-sight vectors if the space receiver's orbit is known. If the orbit is known, then the receiver's position may be estimated with an orbit propagator. Such solutions may experience degradation in accuracy, but the reduction is not significant if the orbit propagation error is small.



Fig. 1 Vectors.

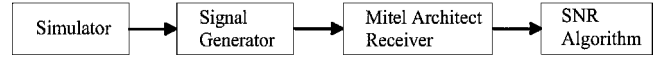
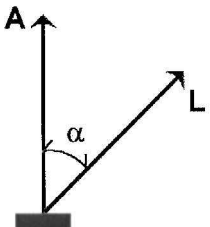


Fig. 2 Simulation setup.

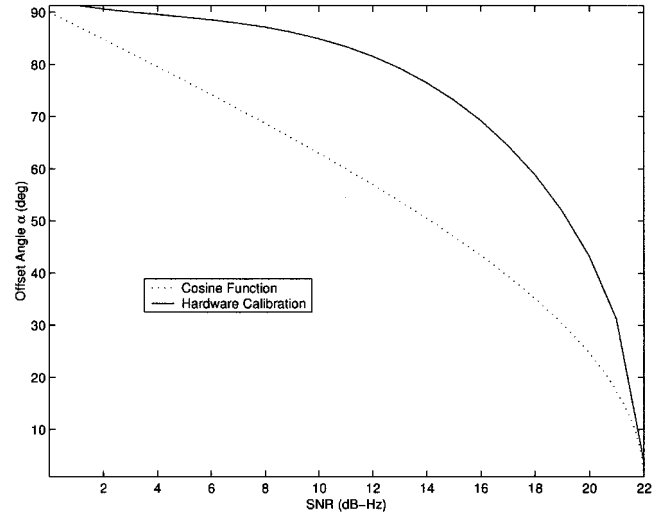


Fig. 3 Calibration line.

The more difficult measurement to obtain is the estimate of the cosine of the angle α from the SNR measurement. The best method of generating this estimate is to perform a hardware calibration on the antenna to be used in the system. This is accomplished by placing the antenna in a known orientation and measuring the reported SNRs and $\cos \alpha$ angles over a period of time. Once a calibration is performed in this manner, a direct estimate of $\cos \alpha$ is available for a given SNR measurement, and no trigonometric functions need to be used. This calibration will be effective as long as the gain pattern of the antenna does not vary significantly from the time of calibration to the time of service. Certain noise sources, such as multipath, may cause the SNR vs α characteristics to be different from the calibration values. As already mentioned, if a calibration cannot be performed, then a cosine function may be used instead.

For this study, a STR 4760 multichannel GPS signal simulator manufactured by Global Systems Simulations, Ltd. (now Spirent Communications) was connected to a Mitel Architect receiver that had been previously modified for space use. The simulator uses GPS satellite orbits and a simulated receiver orbit to calculate GPS signals. These signals included ionosphere effects, measurement noise, and signal strength variations based on a simulated hemispherical antenna receiving pattern. This simulated pattern had maximum signal strength along the boresight vector and a zero signal strength below the local horizon of the antenna. These computed radio frequency signals were then created by the STR-4760 signal generator and fed directly into the GPS receiver through a coaxial cable (Fig. 2). The measurements were obtained at a 1-Hz sample rate. The simulator has the ability to produce multiple antenna outputs, but the Mitel receiver used in this study can only receive one input. Therefore, two Mitel receivers were used. In practice, one receiver with multiple antenna inputs would be a more appropriate system to utilize. An antenna calibration was performed with this setup, and the resulting polynomial curve fit is shown in Fig. 3. As shown, this curve follows the general behavior of a cosine function, although there are some significant differences. Single-vector solutions were generated from SNR measurements using this calibration curve.

Filtering

With some knowledge of the maximum attitude rates expected for the spacecraft platform, the basic SNR algorithm can be improved by passing the measurements through an extended Kalman filter (EKF). The use of the filter prevents poor individual measurements from overly influencing the point solutions. Such poor measurements would cause large solution errors without the presence of the filter. The filter employs a process noise matrix Q to prevent it from

converging to a single solution and, thus, becoming insensitive to attitude maneuvers.

To facilitate the implementation of the filter, the x , y , and z coordinates of the pointing vector solution are first converted into spherical coordinates. The pointing vector solution is expressed in a local vertical/local horizontal reference frame with an azimuth angle θ and an elevation angle ϕ . Thus, all rotations of the frame are due to attitude maneuvers alone and not due to the orbital motion of the spacecraft itself. The measurement model for this filter is the scalar relationship between the measured SNR values and the antenna boresight vector [Eq. (1)] with the boresight vector expressed in spherical coordinates,

$$h = \sin \phi \cos \theta L_x + \sin \phi \sin \theta L_y + \cos \phi L_z \quad (2)$$

Note that Eq. (2) is a scalar relation because single measurements are processed sequentially by the Kalman filter to estimate the boresight direction. The coordinate transformation makes the values of Q directly related to the filter's ability to track attitude maneuvers. With the coordinates changed from Cartesian to spherical, the state vector can be written as

$$X = \begin{bmatrix} \phi \\ \theta \\ \dot{\phi} \\ \dot{\theta} \end{bmatrix} \quad (3)$$

The second two entries in the state vector represent the rate of change of the two spherical coordinates. As a result, some knowledge of the vector pointing solution can be obtained even during periods of signal outage. This choice for the state vector greatly simplifies the state transition matrix, as seen from

$$\Phi = \begin{bmatrix} 1 & 0 & \Delta t & 0 \\ 0 & 1 & 0 & \Delta t \\ 0 & 0 & 1 & 0 \\ 0 & 0 & 0 & 1 \end{bmatrix} \quad (4)$$

Note that for the antenna boresight estimation problem, the state transition matrix is linear. This simplifies the filter design considerably. The standard EKF equations are used (for example, see Gelb,¹⁶ and are repeated here for reference:

$$\hat{x}_i(+) = \hat{x}_i(-) + K_i \{y_i - h[\hat{x}_i(-)]\}$$

$$P_i(+) = [I - K_i H_i [\hat{x}_i(-)]] P_i(-)$$

$$H_i(\hat{x}_i(-)) = \left(\frac{\partial h}{\partial X} \right) \Big|_{X=\hat{x}_i(-)}$$

$$K_i = P_i(-) H_i^T [\hat{x}_i(-)] [H_i(\hat{x}_i(-)) P_i(-) H_i^T + R_i]^{-1} \quad (5)$$

where \hat{x} is the estimated state, K is the filter gain, h is the measurement model, P is the covariance matrix, and R is the measurement weight. The subscript i represents time, and the minus (-) and plus (+) signs are for before and after the measurement update. The state and covariance matrices were propagated forward in time using the state transition matrix already defined and the process noise Q was added to the covariance during the propagation.

The initial guess used for the Kalman filter can greatly affect early performance. To achieve an accurate first guess, the first 10 s of data are processed in a deterministic least-squares algorithm for each epoch. The resulting 10 solutions are then averaged. This solution is used as the first guess for the Kalman filter and filtering then begins.

The SNR algorithm with the Kalman filter was tested under various attitude profiles and with varying Q filter values and measurement weights. For this study, the Euler angle sequence was defined as pitch, roll, and yaw. Pitch is defined as a rotation about the y axis, roll as a rotation about the x axis, and yaw as a rotation about the z axis, where the x , y , and z axes are the local vertical/local horizontal (LV/LH) frame with the x axis pointing along the direction

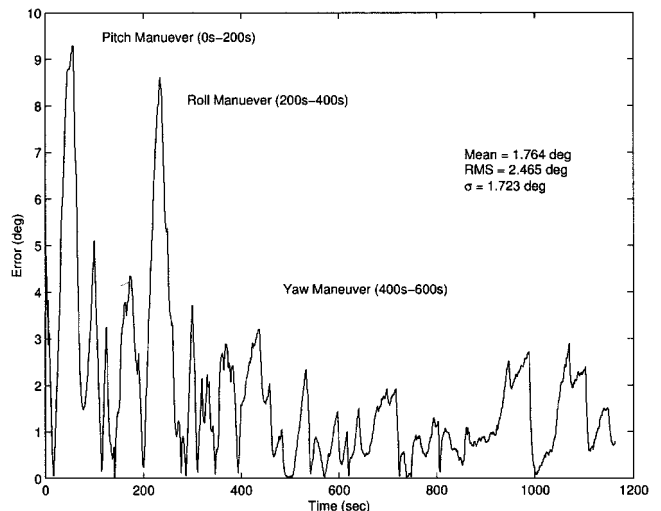


Fig. 4 Filtered estimate for maximum rate configuration.

of flight, the z axis pointed in the local zenith direction, and the y axis completing the right-handed coordinate system. Within this local frame, a nonspinning, zenith pointed, and three-axis stabilized satellite would experience no change in roll, pitch, or yaw.

The results of these tests demonstrate that the filter produces single-vector attitude estimates that are generally accurate to within 10 deg of truth, even during a maximum rate attitude maneuver. For example, one simulation carried out in the International Space Station (ISS) orbit ($a = 66,78,137$ m, $i = 51.6$ deg, and $e = 0.001$) produced the error plot shown in Fig. 4. The antenna was zenith mounted for this test. During this simulation, the vehicle experienced several maximum rate attitude changes of 0.3 deg/s. The vehicle first pitched up at the maximum rate for 100 s, followed immediately by a pitch down over the next 100 s to return to a zenith pointed orientation. This maneuver was then immediately repeated in roll over the next 200 s, followed by the same maneuver in yaw over the following 200 s. After completing these maximum rate attitude maneuvers, the platform remained zenith pointed for the duration of the test. The peak errors of approximately 9 deg occurred during the initial stages of the pitch and roll maneuvers. There was no similar error spike during the yaw maneuver because the zenith pointed antenna cannot detect a change in the yaw angle because the antenna boresight remained constant during this period. The filter equations utilized for this paper assumed that no access to thruster or other attitude maneuvering equipment was available and so all attitude maneuvers were unmodeled in the estimation. The filter equations could be modified if attitude maneuver commands were available and performance would improve. The level of the improvement would be dependent on the accuracy of the dynamic model used.

Three-Axis Solutions

With the single-vector method defined, it is relatively straightforward to extend the SNR algorithm to obtain full three-axis attitude solutions. This modification is accomplished by introducing one or more canted antennas to the system to provide another pointing vector solution. To begin this investigation, one additional antenna was added to the simulation in the layout shown in Fig. 5.

With two antennas, the problem of determining the attitude becomes the traditional problem of generating three-axis attitude solutions from vector observations. This problem has been thoroughly investigated. The optimal attitude solution for this problem is found by minimizing the loss function presented by Wahba¹⁴:

$$L(A) = \frac{1}{2} \sum_{i=1}^n a_i |b_i - A r_i|^2 \quad (6)$$

For this application, unit vectors r_i are the nonrotated antenna boresight vectors, unit vectors b_i are the corresponding results generated by the Kalman filter, a_i are positive weights, and n is the number

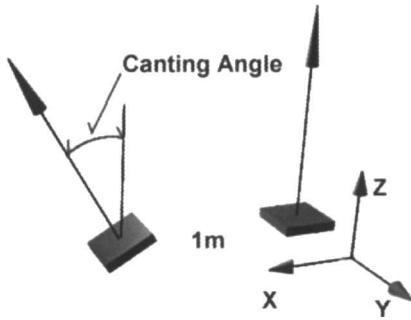


Fig. 5 Antenna layout.

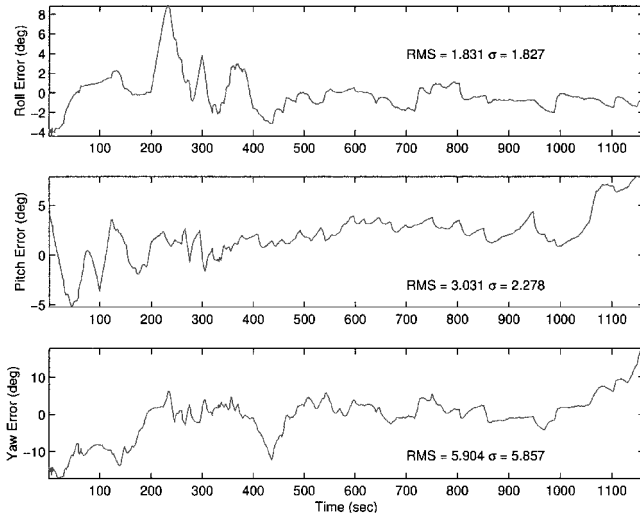


Fig. 6 Attitude errors with two antennas, 30-deg canting angle.

of vector pointing solutions (two in this first experiment). A is the rotation matrix that transforms the nonrotated vectors to the rotated frame.

To compute A , the fast optimal matrix algorithm (FOAM) developed by Markley¹⁷ is utilized. As part of this algorithm, weights can be assigned based on the σ values of the various sensors used. In this problem, the accuracy of the sensor (the SNR measurements) is a function of the geometry of the GPS satellites relative to the antenna boresight vectors. Because the GPS satellites are above the user and the pointing vector solutions improve when multiple GPS satellites are available over a wide range of elevations, this geometry is generally more favorable when the antenna boresight vector is pointed toward the zenith direction. Therefore, weights were assigned based on the square of the cosine of the angle between the estimated vector and zenith. The weights were then normalized so that they all sum to one. This method of assigning the weights improved the three-axis rms error value by 0.5 deg over the case when weights were uniformly assigned to each vector without regard for estimated orientation.

To generate the attitude solutions, the SNR measurements for each antenna were passed through the scalar Kalman filter algorithm, and then the resulting vector solutions were used in the FOAM algorithm, which produced the results. Several simulations were examined to study the performance. As a representative result, the same simulation used for the single-vectorsolution study was considered. Comparing the generated attitude solutions from this simulation to the known truth values produced the error plot shown in Fig. 6. For this simulation, one antenna was canted at 30 deg relative to the zenith pointed antenna, and attitude solutions were generated with the calibration function. This simulation has a total three-axis rms error of 6.89 deg.

As can be seen from Fig. 6, yaw is the least well defined of the three rotation angles. This result is due to the geometry of the antenna layout and the visibility of the corresponding GPS satellites. Yaw accuracy is a function of the offset angle between the two

GPS antennas because only a portion of the information from the offset antenna can be utilized to define the yaw angle. Hence, as the canting angle approaches 90 deg, more of the information from the canted antenna is utilized. The maximum additional information is obtained from this offset antenna when it is canted 90 deg from the original reference antenna. Unfortunately, high canting angles also experience degraded performance because the Earth blocks potential measurements that could be made within the antenna's field of view. To investigate this effect, the simulation was rerun while the canting angle for the second antenna was set at 15 and then 45 deg. As expected, the errors in yaw improved for the 45-deg case and degraded for the 15-deg case. However, there was enough of a degradation in pitch and roll during the 45-deg simulation due to loss of measurements that the 30-deg case had the best three-axis rms accuracy. The case where the antenna was offset 90 deg was also investigated. This case was not desirable because the offset antenna did not obtain sufficient measurements. A summary of these results may be found in Table 1.

A useful feature of this algorithm is its ability to generate rate estimates that may be used during periods of measurement outages. To gain insight into the performance during measurement outages, the rate errors of the vectors are examined over time. These rate errors represent the rate at which the estimated solution deviates from the actual orientation during an outage, assuming no attitude maneuver changes during the outage and excluding the initial offset due to the error in estimated orientation at the time of signal loss. As a result of the three rate maneuvers occurring independent of each other, ϕ_1 represents the pitch and roll rate, whereas θ_2 represents the yaw rate.

Examining the rate error result shows that the errors are greatest over the first few minutes of the simulation. These errors are due primarily to the initialization of the filter. Therefore, they are not a particularly good indication of the filter's performance. If the first 2 min of the simulation are excluded, then the results are more indicative of the actual performance. These results are shown in Fig. 7. In this example, the filter propagates solutions that deviate from the truth at a rate of about 0.2 deg/s. Consequently, some care should be taken when using results generated in this manner, especially over long periods of time.

Table 1 RMS error as a function of canting angle^a

Rotation	Canting angle, deg		
	15	30	45
Roll	2.119	1.831	1.879
Pitch	2.420	3.031	5.863
Yaw	9.381	5.904	5.634
Three axis	9.918	6.885	8.348

^aTwo antennas.

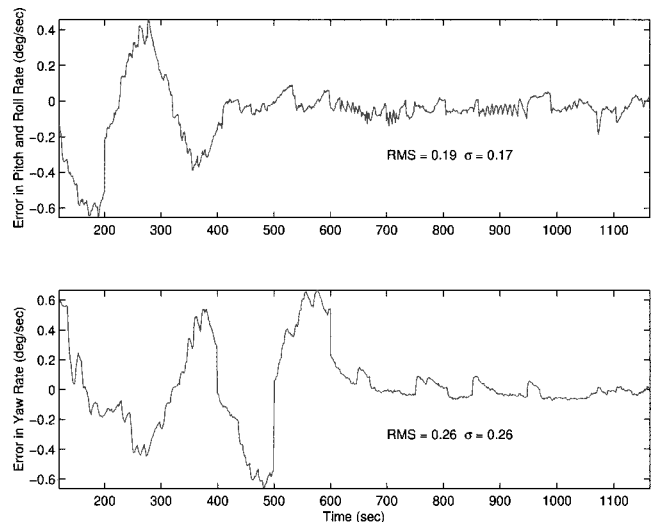


Fig. 7 Rate errors after filter initialization, 30-deg canting angle.

Additional Antennas

One potential goal of this research is to implement an SNR solution method in tandem with a more accurate, if less robust, carrier-phase method. In such a tandem environment, the SNR algorithm would be used with three or four antennas. The solutions generated by the SNR algorithm would be used to initialize the carrier-phase solutions and could be reported as attitude measurements when solutions were unavailable from the more accurate method. To see how the additional antennas improve performance, the same attitude simulations were considered using three and four antennas in a layout similar to a standard-carrierphase array. Each antenna was placed on the corners of a square with 1-m sides. One antenna was zenith pointed whereas the remaining three were each canted in a different direction along the same axis as the sides of the square, as shown in Fig. 8.

The additional antennas improved all of the error measurements and improved the total three-axis rms value by about 1 deg for each additional antenna. The performance of four antennas at a 30-deg canting angle is demonstrated in Fig. 9. A summary of the results using two, three, and four antennas appears in Table 2.

Although it has been shown that a 30-deg canted antenna array is preferable to a 15-deg canted case for the SNR-based attitude solution, it may be possible that a 15-deg case is preferable if carrier-phase measurements are also used. Canting the antennas at larger angles may have several effects on the carrier-phase solution method. The canting angle may affect the performance of the method directly. It has been proposed that circular polarization of the GPS signal may affect the value of the carrier-phase measurement when the antennas are canted relative to each other.¹ It may also be difficult to place antennas at locations that minimize multipath. Additionally, because the carrier-phase method requires that multiple antennas take measurements from the same satellite, it may be beneficial to reduce the canting angle so that more common measurements are generally available. All of these effects may cause the tandem SNR/carrier-phase attitude system to have smaller canting angles than the SNR-only attitude system.

To study the performance in this case, the simulations were run with the antennas canted at 15 deg. As expected, the SNR-only solution accuracy decreased. With four antennas, the total rms value increased from 4.06 to 6.69 deg. If the carrier phase and SNR methods are to be used in tandem, the performance improvement of using

Table 2 RMS error vs number of antennas^a

Rotation	Antennas		
	2	3	4
Roll	1.831	1.637	1.712
Pitch	3.031	2.334	2.046
Yaw	5.904	4.117	3.061
Three axis	6.885	5.058	4.060

^aCanting angle of 30-deg.

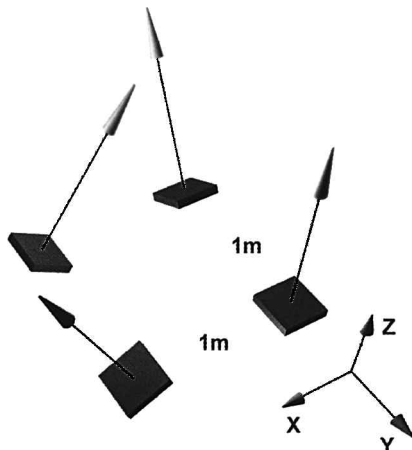


Fig. 8 Four antenna layout, 30-deg canting angle.

Table 3 Static RMS error vs number of antennas^a

Rotation	Antennas		
	2	3	4
Roll	0.938	1.356	0.471
Pitch	3.837	1.752	1.326
Yaw	4.620	3.789	2.670
Three axis	6.078	4.389	3.018

^aCanting angle of 30 deg.

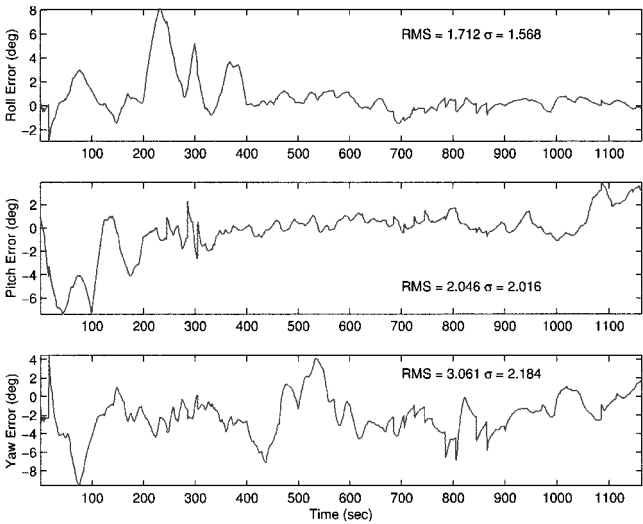


Fig. 9 Attitude estimate error, four antennas, 30-deg canting angle.

the carrier-phases method must be weighed against the degradation in performance of the SNR method when the antennas are less canted to determine the best overall design. The individual application would need to be considered as well.

Whereas the results to this point demonstrate performance during attitude maneuvers and static situations, it is also informative to look at the performance during static situations alone because many applications remain in a static profile over long periods of time. The 30-deg canted case in a static zenith pointed configuration shows considerable improvement in rms error values as compared to the earlier simulation. A summary of these results appears in Table 3.

Computational Expense

This algorithm achieves a relatively minor computational load by utilizing the spherical coordinate system and simplifying the dynamic model. The algorithm was written in MATLAB[®] version 6.5 code and run on a Dell Precision 340 personal computer with a Pentium 4 processor running at 2.2 GHz. For the two, three, and four antenna cases, the algorithm required 9.512, 13.338, and 17.535 s to calculate solutions for all of the data. Over the course of the 1164-s simulation, this works out to an average computational time per 1-s measurement epoch of 0.0082, 0.0115, and 0.0151 s. The largest computational load from the algorithm came from computing dot and cross products. For comparison, running the code on a Dell personal computer with a Pentium 3 processor running at 1.0 GHz required 0.0149, 0.0206, and 0.0268 s of computational time per measurement epoch for the two, three, and four antenna cases.

Error Sources

One advantage of the SNR method is its robustness in the presence of error sources. There are several physical mechanisms that can be expected to produce attitude solution errors in a space environment. Two potentially serious error sources are investigated in this paper, those due to imperfect antenna calibration and those due to sky blockage.

Perhaps the most common source of error for this algorithm could be introduced through an inaccurate antenna calibration function. Errors are introduced through calibration in several ways. Fundamentally, a calibration may not be available at all. If this is the case, a

simple cosine function may be used to estimate the gain pattern. All that is required in this instance is knowledge of the maximum SNR value. This value may be estimated, or the algorithm may be written to rescale the cosine calibration autonomously each time the maximum measured value is increased beyond the previously assumed maximum value. As may be expected, using a cosine function instead of a calibration curve produces an increase in the solution error values. The total rms increased by a factor of 2.5 for the attitude maneuver simulation used in this study. In exchange for this increase in error, however, the use of the cosine function requires no a priori information other than a very general knowledge of the antenna gain pattern to obtain coarse attitude estimates.

A second method of limited calibration is if the calibration operation can only be performed over a short time. This possibility was examined by producing calibration curves using 5-, 10-, and 15-min orbit simulations. These curves were then used in different simulations to study the impact of short calibration times. The results demonstrated that changes in the calibration time had little effect on the solution accuracies generated. A rather short calibration time of 5 min is often sufficient to generate an accurate calibration curve, as long as measurements are taken over a wide range of the antenna gain pattern. This geometry is likely to occur as long as the antenna boresight is nearly zenith pointed during calibration.

In the event that a calibration may be performed in flight, the possibility arises that the true orientation of the platform may not be accurately known. To investigate the effects of an inaccurate known orientation during calibration, calibration curves were generated with errors in the known orientation of 5, 10, and 15 deg. The maneuver profile was then rerun using the resulting curves.

An interesting result is that the performance is not significantly degraded for any of the magnitudes of errors that were introduced in the calibration process. This is likely because during the simulated calibration process the antenna generally experiences a geometry of visible satellites that places them over a wide range of elevations from the erroneous estimated antenna boresight vector. Therefore, over the course of the calibration, the error in the value of $\cos \alpha$ moves through nearly the whole range of its error. This leads to some systematic errors being cancelled out. If the geometry of the satellites is not favorable, as is the case when all of the satellites are on one side of the boresight vector, then performance likely will be impacted more. Unfavorable geometry is more likely to occur as the antenna moves away from a zenith pointed orientation.

These results lead to the possibility that the cosine function could be used during the initial stages of a mission to estimate true orientation. This estimate of truth could then be used to produce a calibration curve. This technique would be possible if the orientation of the spacecraft is near zenith pointed and stable. To investigate this idea, a cosine function was used to estimate the true orientation during a zenith pointed configuration. That information was then used to produce a calibration curve that was used for attitude determination during the maneuver profiles.

The results show that a calibration curve produced by a cosine function can provide results that are as accurate as those produced using a true calibration process. This important result can be used if some outside information is available about the spacecraft during the calibration procedure. As mentioned, the antenna boresight should be nearly zenith pointed and stationary in the LV/LH reference frame over a known period of time. If this is not the case and the cosine function is used to produce a calibration curve, the results may not be as accurate. A summary of the calibration error analysis is presented in Table 4.

A second potential error source is signal outage due to sky blockage from objects in the receiving antenna's field of view. This case was investigated by running scenarios in which various amounts of one or more antenna's field of view was blocked. The results showed that in the ISS orbit, large sections of the sky may be blocked due to obstructions such as the ISS structure itself or nearby orbiting bodies such as the space shuttle, and the solution accuracy is not adversely affected. There is a slight loss of accuracy when three GPS satellites are visible as opposed to four or more, but there is not much change in accuracy with more than four satellites in view.⁹ Therefore, as long as at least four satellites are visible, solution accuracy will be relatively high. In the ISS orbit, nearly one-fourth of the sky can be blocked from the receiving antennas view for a zenith pointed antenna and at least four GPS satellites will still generally be in view.

Conclusions

This work has demonstrated that GPS SNRs may be used with multiple-canted antennas to generate three-axis attitude solutions. When a reasonably accurate model of the antenna gain pattern is used, as obtained through a hardware calibration, an EKF algorithm can provide attitude solutions based on SNRs from two antennas with a three-axis rms accuracy of under 10 deg for a canting angle of 30 deg during attitude maneuvers. During times of measurement outage, the algorithm also provides solutions based on estimated angular rates. These solutions deviate from the truth at a nearly constant rate, and some care should be taken when using estimates generated in this manner. When the number of antennas utilized increases to four, the accuracy level increases to a three-axis rms value of 4 deg. This value improves further during static attitude profiles to a three-axis rms value of 3 deg.

In addition to providing solutions, the new algorithm was demonstrated to be relatively robust in the presence of error sources. The greatest risk factor studied for this algorithm was the introduction of errors during the calibration process. One possible calibration procedure would be to calibrate the antenna on the ground using sky data with the antenna mounted on the satellite or on a model of the satellite. Such a calibration would allow some of the effects of multipath due to the satellite configuration to be determined. Such a preflight calibration must, however, allow for possible changes in the maximum SNR because the signal strengths are likely to increase once in space. To obtain the best possible performance, an in-flight calibration process should be performed while the vehicle is in a known and nearly zenith pointed orientation. If the vehicle attitude is not perfectly known during calibration, the performance is not affected much by using an estimate of the true orientation within 15 deg of the truth. This type of accuracy can be realized by using a cosine function to estimate truth as long as the spacecraft is nearly zenith pointed and does not experience any large attitude maneuvers during the calibration interval.

If a calibration cannot be performed, solutions may still be generated using a self-scaling cosine function in lieu of the calibration curve. When such a cosine function is used, the algorithm requires no a priori information to generate attitude solutions. Solutions generated in this manner, however, will be less accurate than those generated with a calibration curve.

The results of this analysis lead to the conclusion that a three-axis attitude solution based on SNR measurements may be used to provide attitude determination from GPS receivers without many of the limitations of traditional carrier-phase methods. The algorithm is both simple to implement and robust to error sources.

This SNR algorithm could be used in tandem with a more accurate carrier-phase method to provide solutions at times when the more accurate solutions are unavailable, thus, providing a complete system that provides both accurate solutions and a maximum amount of total solution coverage. To make this system design possible, the task of modifying a carrier-wave solution method to account for canted antennas must be accomplished. This will require additional study and research. Additionally, this SNR algorithm could significantly reduce the search space required for the ambiguity resolution procedure. The accuracy levels demonstrated in this analysis lead to the possibility of reducing the search space to only a few integers in

Table 4 RMS error vs calibration type^a

Rotation	Calibration type		
	Cosine function	5-min calibration time	Truth estimated via cosine function
Roll	4.167	1.627	1.852
Pitch	4.688	1.723	2.054
Yaw	8.344	3.240	3.046
Three axis	10.438	4.014	4.114

^aFour antennas, 30-deg canting angle.

many cases. This could significantly improve the initialization time and success rate of the carrier-phase methods.

Even with only two antennas, the solution accuracy of this analysis is satisfactory for many applications. Future work will be done with rooftop experiments to validate this performance. Such a test will also better quantify any effects due to physical error sources such as multipath. On completion of these tasks, a GPS attitude determination system will be available that can accurately determine attitude during most of the mission stages encountered during a spacecraft's mission life, given that GPS satellites are in view. This system provides a versatile and cost-effective solution to many spacecraft attitude determination problems.

Acknowledgments

The authors acknowledge the support of Kevin Key and Takuji Ebinuma. K. Key modified the Mitel receiver to make it usable in space and T. Ebinuma wrote the receiver code that generated the line-of-sight vectors and the signal-to-noise ratio measurement outputs. Their assistance is appreciated.

References

- ¹Lightsey, E. G., "Development and Flight Demonstration of a GPS Receiver for Space," Ph.D. Dissertation, Dept. Aeronautics and Astronautics, Stanford Univ., Stanford, CA, Feb. 1997.
- ²Axelrad, P., and Ward, L. M., "Spacecraft Attitude Estimation Using the Global Positioning System: Methodology and Results for RADCAL," *Journal of Guidance, Control, and Dynamics*, Vol. 19, No. 6, 1996, pp. 1201–1209.
- ³Carpenter, J. R., and Hain, R. M., "Precise Evaluation of Orbital GPS Attitude Determination on the STS-77 GPS Attitude and Navigation Experiment (GANE)," *Proceedings of the ION National Technical Meeting*, Inst. of Navigation, Fairfax, VA, 1997, pp. 387–398.
- ⁴Brock, J. K., Fuller, R., Kemper, B., Mlezcko, D., Rodden, J., and Tadros, A., "GPS Attitude Determination and Navigation Flight Experiment," *Proceeding of the ION GPS*, Inst. of Navigation, Fairfax, VA, 1995, pp. 545–554.
- ⁵Ward, L. M., "Spacecraft Attitude Estimation Using GPS: Methodology and Results," Ph.D. Dissertation, Dept. Aerospace Engineering Science, Univ., Colorado, Boulder, CO, Aug. 1996.
- ⁶Melvin, P. J., Ward, L. M., and Axelrad, P., "The Analysis of GPS Attitude Data from a Slowly Rotating, Symmetrical Gravity Gradient Satellite," *Journal of Astronautical Sciences*, Vol. 44, No. 4, Oct./Dec. 1996, pp. 515–539.
- ⁷Ward, L. M., and Axelrad, P., "A Combined Filter for GPS-Based Attitude and Baseline Estimation," *Navigation: Journal ION*, Vol. 44, No. 2, 1997, pp. 195–213.
- ⁸Lightsey, E. G., Campbell, C. E., Carpenter, R., Simpson, J., and Davis, G., "Design and Performance of Space Algorithms for the GPS Receiver Used on International Space Station and Crew Return Vehicle," *International Workshop on Aerospace Applications of the Global Positioning System*, International Federation on Automatic Control, Laxenburg, Austria, 2000.
- ⁹Madsen, J. D., and Lightsey, E. G., "Kalman Filtered Signal to Noise Ratio Pointing Vector Algorithm for the Space Station," *Proceedings of the ION National Technical Meeting*, Inst. of Navigation, Fairfax, VA, 2001, pp. 133–143.
- ¹⁰Axelrad, P., and Behre, C. P., "Satellite Attitude Determination Based on GPS Signal-to-Noise Ratio," *Proceedings of the IEEE*, Vol. 87, No. 1, 1999, pp. 122–144.
- ¹¹Dunn, C., and Duncan, C., "Estimating Attitude From GPS Measurements on one Antenna," NASA Technical NPO 20323 Briefs, June 1998.
- ¹²Buist, P. J., Hashida, Y., Unwin, M., and Schroeder, M., "Spacecraft Full Attitude Determination from a Single Antenna: Experimentation with the PoSAT-1 GPS Receiver," *Proceedings of the ION Technical Meeting*, Inst. of Navigation, Fairfax, VA, 1998, pp. 1811–1817.
- ¹³Serrano, J., Potti, J., Bemede, P., and Silvestrin, P., "New Spacecraft Attitude Determination Scheme Based on the Use of GPS Line-of-Sight Vectors," *Proceedings of the ION GPS-95*, Inst. of Navigation, Fairfax, VA, 1995, pp. 1797–1806.
- ¹⁴Wahba, G., "A Least Squares Estimate of Spacecraft Attitude," *SIAM Review*, Vol. 7, No. 3, 1965, p. 409.
- ¹⁵Pasetti, A., Gottifredi, F., and Colmenarejo, P., "A Visibility-based Algorithm for the GPS Initial Integer Ambiguity Problem," *Proceedings of the 3rd International ESA Conference on Spacecraft GNC*, ESA, Noordwijk, The Netherlands, 1996, pp. 327–333.
- ¹⁶Gelb, A., *Applied Optimal Estimation*, MIT Press, Cambridge, MA, 1994, p. 188.
- ¹⁷Markley, F. L., "Attitude Determination Using Vector Observations: A Fast Optimal Matrix Algorithm," *Journal of the Astronautical Sciences*, Vol. 31, No. 2, 1993, pp. 261–280.